Article

Not peer-reviewed version

Lipid-Associated Morphotypes in *Leishmania* Promastigotes and Amastigotes Reflect Parasite Microdiversity in an Amazonian Transmission Landscape

Áurea Martins Gabriel *, Gilvando Galvão, Adan Galué-Parra, Washington Luiz Assunção Pereira, Ketil Winther Pedersen, Delia Cristina Figueira Aguiar, Evonnildo Costa Gonçalves, Edilene Oliveira da Silva

Posted Date: 26 May 2026

doi: 10.20944/preprints202605.1750.v1

Keywords: *Leishmania amazonensis*; lipid-associated morphotypes; lipid-rich structures; lipid droplets; ultrastructure; transmission electron microscopy; scanning electron microscopy; BODIPY® staining; intracellular amastigotes; parasitophorous vacuole; membrane-associated compartments; parasite microdiversity; Amazonian endemic areas

 doi:10.20944/preprints202605.1750.v1

Article

Lipid-Associated Morphotypes in *Leishmania* Promastigotes and Amastigotes Reflect Parasite Microdiversity in an Amazonian Transmission Landscape

Áurea Martins Gabriel [1,2,*], Gilvando Rodrigues Galvão [3], Adan Galué-Parra [2], Washington Luiz Assunção Pereira [4], Ketil Winther Pedersen [5], Délia Cristina Figueira Aguiar [2], Evonnildo Costa Gonçalves [2] and Edilene Oliveira da Silva [2,6]

[1] Global Health and Tropical Medicine (GHTM), Institute of Hygiene and Tropical Medicine, NOVA University of Lisbon (IHMT-UNL), 1349-008 Lisbon, Portugal
[2] Institute of Biological Sciences, Federal University of Pará (UFPA), Av. Augusto Correa 01, 66075-110 Belém, PA, Brazil
[3] Veterinary Hospital Mário Dias Teixeira, Federal Rural University of Amazon, UFRA, 66077-830 Belém, PA, Brazil
[4] Laboratory of Animal Pathology, Federal Rural University of Amazon (UFRA), 66077-830 Belém, PA, Brazil
[5] Thermo Fisher Scientific, 0379 Oslo, Norway
[6] National Center for Structural Biology and Bioimaging (CENABIO), 21941-902 Rio de Janeiro, RJ, Brazil
* Correspondence: aurea.gabriel@ihmt.unl.pt or aureamartins@ufpa.br

Simple Summary

Leishmania parasites rely on lipids and membrane-based structures to survive in diverse environments, including within host macrophages. Using multiple microscopy approaches, we examined how lipid-rich and vesicle-like compartments are organized in two life stages of *Leishmania amazonensis*: promastigotes and intracellular amastigotes. Each stage displayed distinct lipid-associated structures, and particle analysis of culture supernatants revealed marked differences in abundance and size distribution. Although we do not infer biological function, these descriptive observations provide a structural baseline for understanding membrane organization in *Leishmania*. When considered alongside previously reported genetic microdiversity in Amazonian parasite populations, our findings suggest that subtle genetic variation may contribute to morphological heterogeneity. This work supports future research on parasite adaptation, host–parasite interactions, and potential therapeutic targets.

Abstract

Lipid-rich and vesicle-like structures are recurrent features of *Leishmania* spp., yet their morphological diversity and stage-specific organization remain incompletely defined. Here, we provide a descriptive ultrastructural and fluorescence-based characterization of lipid-associated compartments in *Leishmania (L.) amazonensis* promastigotes and intracellular amastigotes using transmission electron microscopy, scanning electron microscopy, BODIPY® staining, and Nanoparticle Tracking Analysis (NTA). Promastigotes displayed electron-dense lipid bodies adjacent to the Golgi complex and abundant vesicle-like profiles within the flagellar pocket, whereas intracellular amastigotes exhibited rounded lipid-rich inclusions within parasitophorous vacuoles. NTA revealed stage-dependent differences in particle abundance and size distribution, interpreted strictly at the descriptive level in accordance with MISEV2023 guidelines. These findings establish a morphological baseline for lipid-associated structures across parasite stages. When contextualized with previously reported low-level genetic polymorphisms in Amazonian *Leishmania* populations, the observed structural heterogeneity suggests that microdiversity may contribute to variation in

 doi:10.20944/preprints202605.1750.v1

vacuolar lipid organization. This framework provides a foundation for future studies integrating ultrastructure, lipidomics, and parasite genomics.

Keywords: *Leishmania amazonensis*; lipid-associated morphotypes; lipid-rich structures; lipid droplets; ultrastructure; transmission electron microscopy; scanning electron microscopy; BODIPY® staining; intracellular amastigotes; parasitophorous vacuole; membrane-associated compartments; parasite microdiversity; Amazonian endemic areas

1. Introduction

Leishmaniases are vector-borne zoonotic diseases caused by protozoa of the genus *Leishmania*, which display remarkable ecological plasticity and the ability to infect a wide range of mammalian hosts [1,2]. Their digenetic life cycle alternates between extracellular promastigotes in phlebotomine sand flies and intracellular amastigotes within mammalian macrophages [3]. In the Americas, transmission is driven primarily by *Lutzomyia longipalpis* in visceral leishmaniasis and by several *Psychodopygus* species in cutaneous forms [4,5]. The Amazon Basin represents one of the most complex transmission systems worldwide, shaped by rapid environmental change, urban expansion, and the coexistence of domestic, synanthropic, and wild reservoirs [6–8].

Dogs are the principal domestic reservoir of *Leishmania (L.) infantum*, playing a central role in the maintenance and amplification of transmission [9–11]. Clinical manifestations in dogs range from asymptomatic infection to severe systemic disease, reflecting the interplay between parasite virulence, host immune responses, and ecological context [12,13]. Diagnostic challenges persist in endemic areas where multiple *Leishmania* species co-circulate and asymptomatic infections are common [14,15].

At the cellular level, *Leishmania* parasites rely on highly specialized membrane-trafficking pathways, including the flagellar pocket—the exclusive site of endocytosis and exocytosis [16,17]—and the formation of lipid-associated structures that support survival within host macrophages. Lipid droplets (LDs) and vesicle-like compartments have been increasingly recognized as key components of parasite–host communication [18–20]. Recent studies have shown that *Leishmania* extracellular vesicles (EVs) carry lipids, proteins, and nucleic acids capable of modulating host immunity [21–23], while lipid remodeling contributes to parasite adaptation, virulence, and drug resistance [24–26]. In macrophages, infection by *L. amazonensis* induces LD biogenesis and inflammatory lipid mediator production [27], highlighting the importance of lipid-associated processes in intracellular survival.

Ultrastructural studies have documented heterogeneous membrane-bound profiles in promastigotes, including tubular and vesicular elements within the flagellar pocket [16,17], and megasomes in amastigotes, which participate in vacuolar remodeling and proteolysis [28]. However, the morphology, distribution, and developmental regulation of lipid-associated compartments in *Leishmania* amastigotes remain poorly defined. This gap is particularly relevant in the Amazonian context, where molecular analyses have revealed low-level nucleotide polymorphisms and mosaic aneuploidy in *L. infantum*, suggesting the circulation of genetically distinct parasite clones [8,29].

In this study, we integrate ultrastructural analyses of *L. amazonensis* promastigotes and intracellular amastigotes with molecular and epidemiological data from naturally infected dogs in Pará, Brazil. By combining transmission electron microscopy, scanning electron microscopy, neutral-lipid staining, and dual-marker molecular diagnostics, we aim to (i) characterize lipid-associated structures across parasite stages, (ii) contextualize these findings within real-world transmission settings, and (iii) explore potential links between parasite microdiversity and morphological variation. This integrated approach provides a refined structural baseline for future lipidomic, biochemical, and functional studies on parasite adaptation within host cells.

 doi:10.20944/preprints202605.1750.v1

2. Materials and Methods

2.1. Study Context and Epidemiological Framework

The ultrastructural analyses presented in this study were contextualized using epidemiological and molecular data from natural canine infections in three endemic municipalities of Pará, northern Brazil—Belém, Marabá, and Colares. These areas represent distinct transmission settings shaped by urban expansion, environmental modification, and the presence of competent vectors vectors (*Lutzomyia longipalpis* for visceral leishmaniasis and *Psychodopygu*s spp. for cutaneous transmission in the Amazon basin) [1–4]. Between 2007 and 2017, Pará reported more than 42,000 human cases of leishmaniasis, including 3,786 cases of visceral disease, reflecting substantial spatial heterogeneity across municipalities [5]. Previous molecular surveys of 130 dogs from these regions revealed infection prevalences of 76% in Marabá, 53.1% in Belém, and 35.5% in Colares, with *Leishmania (L.) infantum* identified as the sole circulating species [6]. These data provide the epidemiological foundation for interpreting the ultrastructural and molecular findings described herein.

2.2. Canine Population and Clinical Characterization

A total of 130 domestic dogs from Belém, Marabá, and Colares were included in this study as part of routine epidemiological surveillance. Animals were recruited during clinical examinations conducted in municipal veterinary units and field campaigns in endemic neighborhoods. For each dog, a standardized clinical assessment was performed, including complete physical examination and classification into symptomatic or asymptomatic categories based on the presence of at least two clinical signs compatible with canine leishmaniasis (e.g., weight loss, lymphadenopathy, alopecia, cutaneous lesions, onychogryphosis).

Demographic variables (age, sex, and breed) were recorded to evaluate potential associations with infection status. Biological samples were collected using minimally invasive procedures: (i) EDTA-treated whole blood, obtained by jugular venipuncture; and (ii) conjunctival swabs, collected by gently rotating sterile swabs over the ocular mucosa.

All samples were transported under refrigeration and processed immediately or stored at −20 °C until molecular analysis. This sampling strategy ensured high diagnostic sensitivity while minimizing animal discomfort and enabling the inclusion of both symptomatic and asymptomatic dogs.

2.3. Molecular Detection of Leishmania spp.

DNA was extracted from whole blood using commercial kits and from conjunctival swabs using NaCl-based extraction protocols (salting-out method). Two molecular markers were targeted: (i) the small subunit ribosomal RNA gene (SSU rDNA) using nested PCR, and (ii) kinetoplast minicircle DNA (kDNA) using species-specific primers for *L. infantum* [6–8].

PCR products were visualized on agarose gels stained with nucleic acid dye. Positive SSU rDNA amplicons were purified and sequenced using BigDye® Terminator chemistry on an ABI 3500XL platform. Sequences were edited, aligned, and compared with GenBank entries using BLASTn. Single nucleotide polymorphisms (SNPs) and insertions/deletions were identified, and phylogenetic relationships were inferred using the Neighbor-Joining method with 2,000 bootstrap replicates [6,9].

2.4. Statistical Analysis of Natural Infection Data

Associations between infection status and clinical or demographic variables were evaluated using chi-square tests, with significance set at $p < 0.05$. Odds ratios (OR) and 95% confidence intervals (CI) were calculated. Agreement between sample types (blood vs. swab) and between molecular markers (kDNA vs. SSU rDNA) was assessed using contingency tables [6].

 doi:10.20944/preprints202605.1750.v1

2.5. Parasite Culture and Preparation for Ultrastructural Analysis

Promastigote forms of *Leishmania (L.) amazonensis* (strain MHOM/BR/26361) were cultured in RPMI 1640 supplemented with 10% fetal bovine serum at 27 °C. Parasites were harvested at exponential and stationary phases, counted in a Neubauer chamber, and processed for microscopy following established protocols [10–12]. These procedures are consistent with classical promastigote ultrastructural studies describing Golgi-associated cisternae, flagellar pocket organization, and endomembrane dynamics [13–15].

2.6. Macrophage Isolation and Infection Assays

Peritoneal macrophages were obtained from male BALB/c mice (6–8 weeks old) following CONCEA guidelines (CEUA/UFPA protocol 4847221118). Cells were seeded on glass coverslips, allowed to adhere, and infected with stationary-phase promastigotes at a 10:1 parasite-to-cell ratio. After removal of non-internalized parasites, cultures were incubated for 24–72 h before fixation [16]. This model is widely used for studying intracellular amastigotes and vacuolar remodeling [17,18].

2.7. Transmission Electron Microscopy (TEM)

Promastigotes and infected macrophages were fixed in glutaraldehyde/paraformaldehyde, post-fixed in osmium tetroxide with potassium ferrocyanide, dehydrated in graded acetone, embedded in Epon®, sectioned, and contrasted with uranyl acetate and lead citrate. Samples were examined using a LEO 906 E transmission electron microscope. Tissue samples from experimentally infected BALB/c mice were processed using identical fixation and embedding protocols [14–16]. This workflow preserves membrane-associated structures, including lipid droplets, megasomes, and vacuolar inclusions, as described in classical and recent ultrastructural studies [19–21].

2.8. Scanning Electron Microscopy (SEM)

Promastigotes and infected macrophages were fixed, dehydrated in ethanol, critical-point dried, sputter-coated with gold, and imaged using a MIRA 3 TESCAN scanning electron microscope. For visualization of intracellular amastigotes, the apical macrophage surface was gently removed to expose parasitophorous vacuoles [22]. SEM imaging complements TEM by revealing surface topology and vacuolar architecture [23].

2.9. Neutral-Lipid Staining

Promastigotes and infected macrophages were stained with BODIPY® 493/503 to visualize neutral-lipid pools. Samples were imaged using fluorescence microscopy with FITC and DAPI filters. Staining was used exclusively for qualitative assessment, in accordance with MISEV2023 recommendations [24]. BODIPY® staining is widely used to detect lipid droplets in trypanosomatids and host cells [25,26].

2.10. Nanoparticle Tracking Analysis (NTA)

Extracellular particles from promastigote and amastigote preparations were analyzed using a 488-nm laser-equipped NTA system. Particle size distribution and concentration were recorded. As intracellular amastigotes remain confined within parasitophorous vacuoles, extracellular particles in amastigote cultures were interpreted as host-derived. No inference regarding vesicle identity, biogenesis, or function was attempted [22,24]. NTA is a biophysical method that cannot distinguish EVs from non-vesicular particles, especially in complex biological systems [28–30].

 doi:10.20944/preprints202605.1750.v1

3. Results

3.1. Epidemiological and Molecular Context of Natural Infections

A total of 130 dogs from three municipalities of Pará (Belém, Marabá, and Colares) were evaluated. Infection prevalence varied markedly across locations: 76.0% in Marabá (95% CI: 61.9–86.8%), 53.1% in Belém (95% CI: 38.7–67.1%), and 35.5% in Colares (95% CI: 19.8–53.6%) [6]. These non-overlapping confidence intervals highlight the pronounced epidemiological heterogeneity across the Amazonian transmission landscape. Clinical evaluation further revealed that 90.3% of infected animals were symptomatic, whereas only 21.5% of non-infected dogs exhibited compatible signs ($\chi^2 = 25.80$, $p < 0.001$; OR = 9.95; 95% CI: 3.92–25.3), indicating a strong association between clinical status and infection. No significant associations were observed between infection status and age, sex, or breed. Collectively, these findings reflect the heterogeneous transmission dynamics of the Amazon and align with previous epidemiological surveys documenting high canine infection rates preceding human cases [14–16].

3.2. Detection of Leishmania DNA in Different Biological Samples

Among the 130 dogs evaluated, 58 (44.6%) were positive for *Leishmania* DNA in blood samples and 54 (41.5%) in conjunctival swabs. Concordance between sample types was moderate: 33.1% of animals were positive in both matrices, whereas 25.9% were positive only in blood and 15.3% only in swabs ($\chi^2 = 43.44$, $p < 0.001$). Agreement analysis confirmed a moderate level of reliability between the two sampling approaches ($\kappa = 0.59$, $p < 0.001$), with an observed concordance of 80%. These findings indicate that blood and conjunctival swabs provide complementary diagnostic information, supporting the use of non-invasive sampling strategies for canine leishmaniasis, as reported in previous studies [17].

3.3. Sensitivity of Molecular Markers

The two molecular markers employed—kDNA minicircle PCR and SSU rDNA nested PCR—showed comparable sensitivity for detecting *Leishmania* infection. Although kDNA identified a slightly higher number of positive samples, no statistically significant difference was observed between markers, supporting their combined use for robust detection in field conditions [6].

3.4. Genetic Variability Among Circulating Strains

Sequencing of SSU rDNA amplicons confirmed *Leishmania (L.) infantum* as the sole circulating species across all municipalities. Four sequences exhibited nucleotide variation, including three with degenerate bases and one with a pyrimidine transition (C→T). These low-level polymorphisms suggest the presence of genetically distinct parasite clones circulating within the same endemic area, consistent with microdiversity and mosaic aneuploidy described in *Leishmania* populations [8,30].

3.5. Ultrastructure of Promastigotes

Transmission electron microscopy revealed the classical morphology of *L. amazonensis* promastigotes, including an elongated cell body, a single anterior flagellum, and a well-defined flagellar pocket. Lipid-rich compartments appeared as rounded, electron-dense droplets located near the Golgi complex and adjacent to the flagellar pocket (Figure 1). These structures corresponded to the punctate neutral-lipid staining observed with BODIPY® 493/503.

Vesicle-like profiles were frequently observed within the flagellar pocket, consistent with its role as the exclusive site of endocytosis and exocytosis in *Leishmania* [31–33]. These observations align with classical descriptions of flagellar pocket trafficking and membrane turnover in trypanosomatids [31–33].

 doi:10.20944/preprints202605.1750.v1

Scanning electron microscopy confirmed the fusiform shape of promastigotes and did not reveal prominent surface protrusions suggestive of active extracellular vesicle budding under the conditions tested.

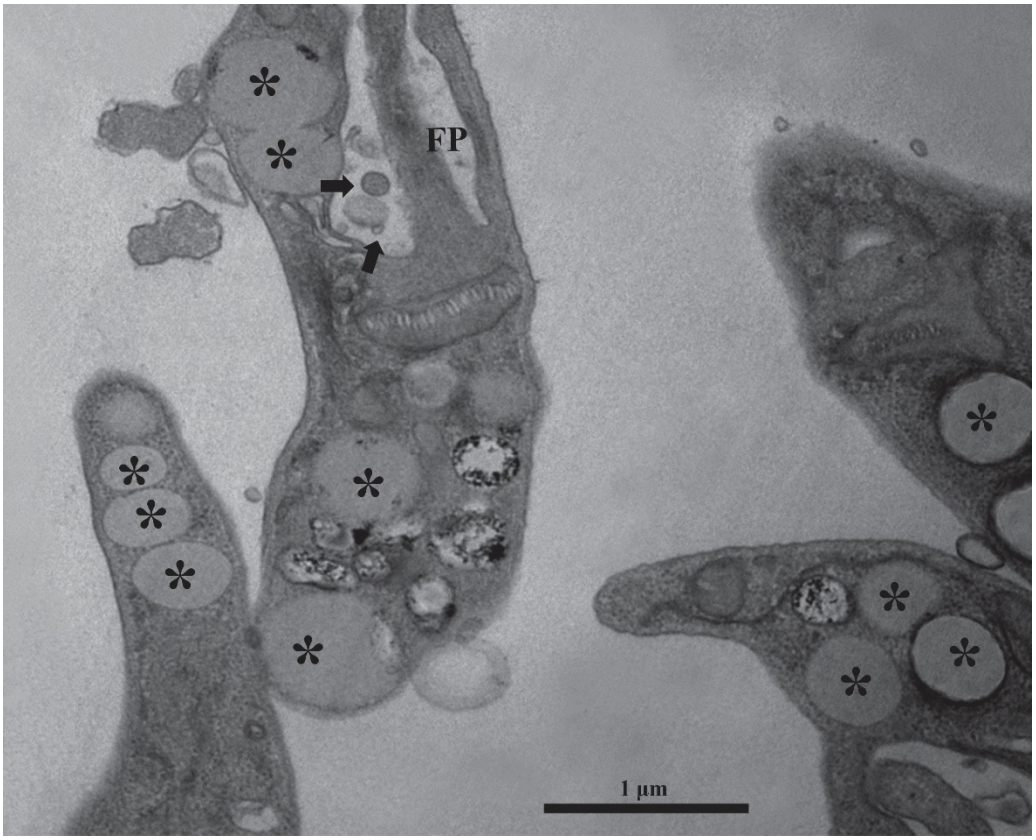

Figure 1. Transmission electron microscopy of *Leishmania (L.) amazonensis* promastigotes. (A–C) Classical promastigote morphology showing an elongated cell body, a single anterior flagellum, and a well-defined flagellar pocket. (D–F) Lipid-rich compartments appearing as rounded, electron-dense lipid droplets (arrows) located near the Golgi complex and adjacent to the flagellar pocket. These membrane-associated structures are consistent with previous ultrastructural descriptions in *Leishmania* spp. Scale bars: 1 µm.

3.6. Ultrastructure of Intracellular Amastigotes

Intracellular amastigotes were observed within large parasitophorous vacuoles of infected macrophages. TEM revealed rounded inclusions of variable electron density within the vacuolar lumen, distinct from the cytoplasmic lipid droplets observed in promastigotes (Figure 2). These inclusions were frequently positioned near the amastigote surface or associated with host-derived membranes and were compatible with lysosomal-related compartments, including megasomes described in *Leishmania* spp. [21,31–33].

SEM imaging of infected macrophages, after removal of the apical surface, exposed enlarged parasitophorous vacuoles containing multiple amastigotes and heterogeneous luminal material (Figure 3). These observations are consistent with vacuolar remodeling processes as previously described in intracellular trypanosomatids [17,18].

 doi:10.20944/preprints202605.1750.v1

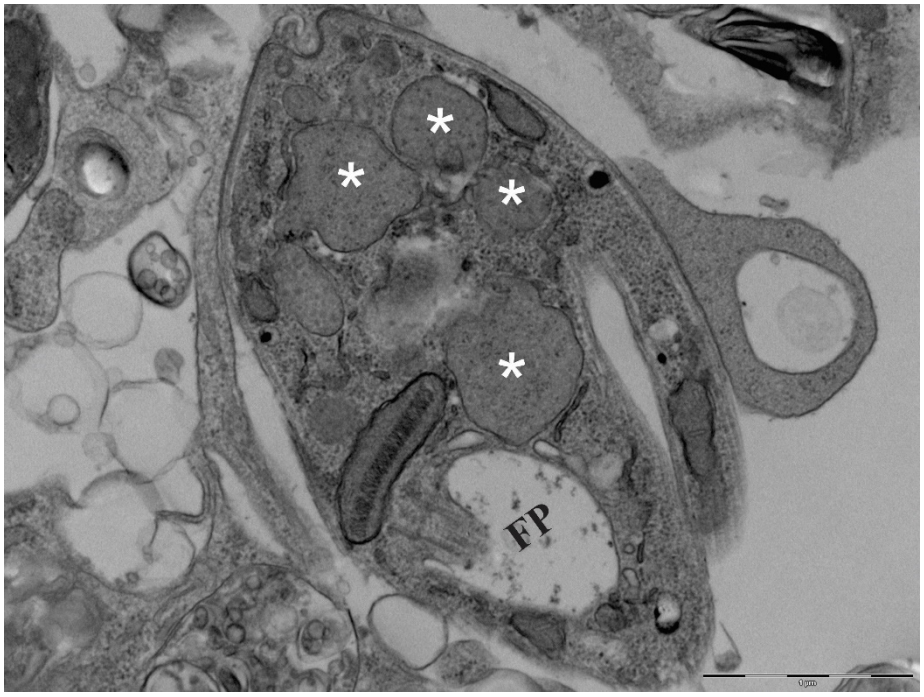

Figure 2. Transmission electron microscopy of intracellular *L. amazonensis* amastigotes within parasitophorous vacuoles. (A–C) Amastigotes enclosed within large parasitophorous vacuoles of infected macrophages. (D–F) Rounded inclusions (arrowheads) located in the vacuolar lumen, distinct from the cytoplasmic lipid droplets observed in promastigotes. These structures display variable electron density and are frequently positioned near the amastigote surface or associated with host-derived membranes. Scale bars: 1 µm.

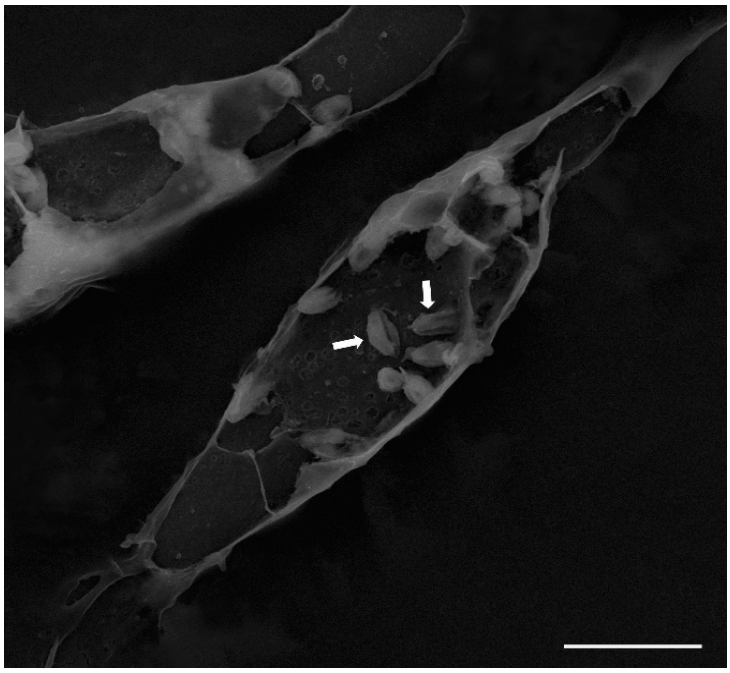

Figure 3. Scanning electron microscopy of infected macrophage after apical surface removal. (A) Promastigote morphology showing a fusiform cell body and a single emergent flagellum. (B–D) Parasite-containing parasitophorous vacuoles exposed after gentle tape stripping. Multiple intracellular amastigotes (arrows) are visible within enlarged vacuoles 72 h post-infection. Scale bars: 10µm. (Heterogeneous vacuolar material is consistent with TEM observations).

 doi:10.20944/preprints202605.1750.v1

3.7. Neutral-Lipid Staining

BODIPY® 493/503 staining of promastigotes revealed discrete cytoplasmic puncta consistent with neutral lipid droplets. Flow cytometry profiles of BODIPY-labeled promastigotes are shown in Figure 4, and representative fluorescence micrographs are presented in Figure 5. In infected macrophages, diffuse BODIPY® fluorescence was detected within parasitophorous vacuoles, with occasional puncta adjacent to intracellular amastigotes. These observations highlight the stage-specific organization of lipid-associated compartments in *Leishmania* [25,26].

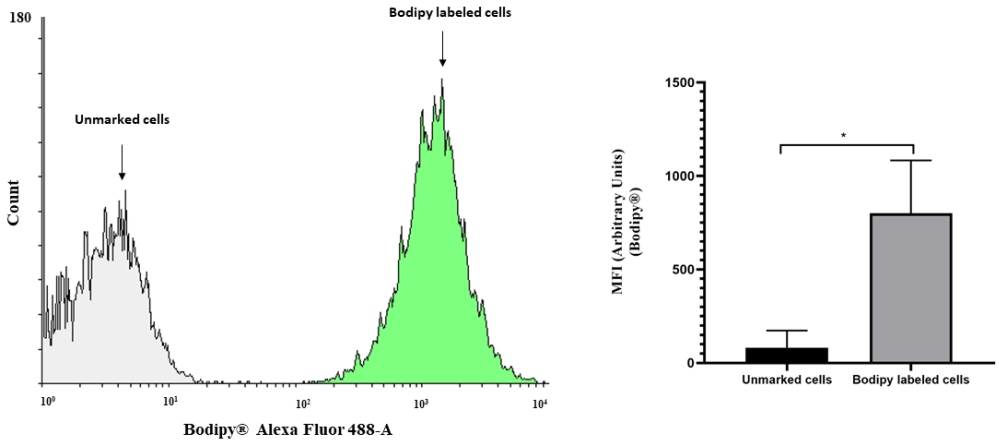

Figure 4. Flow cytometry analysis of BODIPY®-labeled *Leishmania (L.) amazonensis* promastigotes. (A) Histogram showing fluorescence intensity detected in the Alexa Fluor 488-A channel for unmarked cells (gray) and BODIPY®-labeled cells (green). (B) Mean fluorescence intensity (MFI) of unmarked and labeled cells. Labeled promastigotes exhibited significantly higher fluorescence (***p < 0.001; ANOVA with Tukey post-hoc test). Fluorescence values were interpreted strictly at the descriptive level.

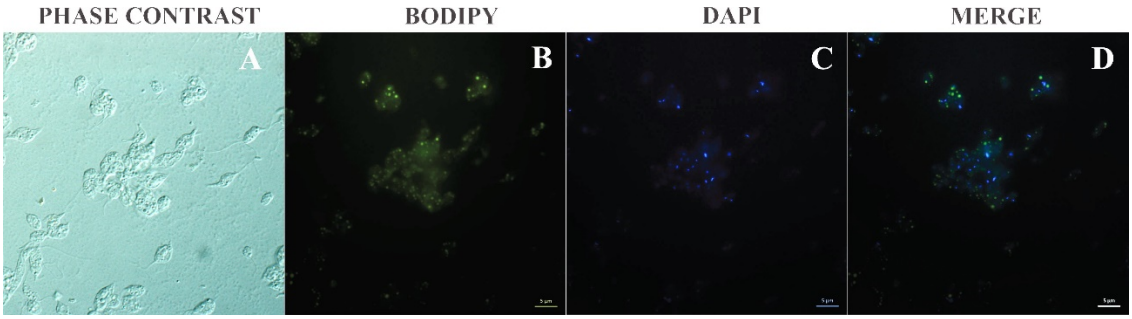

Figure 5. BODIPY® 493/503 staining of neutral-lipid pools in promastigotes. (A) Phase-contrast image. (B) BODIPY-labeled neutral lipid bodies appearing as discrete cytoplasmic puncta. (C) DAPI-stained nucleus. (D) Merged image showing the spatial relationship between nuclear and lipid signals. The punctate fluorescence pattern corresponds to the ultrastructural localization of lipid droplets. Scale bars: 5 μm.

3.8. Nanoparticle Tracking Analysis

NTA of culture supernatants revealed heterogeneous submicron particle populations in both promastigote and amastigote preparations. NTA values are interpreted strictly as biophysical descriptors of particle size and concentration. As intracellular parasites remain confined within parasitophorous vacuoles, extracellular particles in amastigote cultures likely originate from host cells. In accordance with MISEV2023, no inference regarding vesicle identity, biogenesis, or function was attempted [22].

 doi:10.20944/preprints202605.1750.v1

NTA profiles were consistent with previous reports describing polydisperse extracellular particle populations in trypanosomatid cultures, where non-vesicular particles, protein aggregates, and membrane fragments coexist [28–31].

A comparative summary contrasting the present ultrastructural findings with previously reported host-directed lipid studies is presented in Table 1. Both the current analyses and the earlier studies—each conducted in our laboratory—are positioned side-by-side to delineate methodological continuity and conceptual distinctions.

Table 1. Comparative framework between the present ultrastructural study and the crotoxin-modulated macrophage lipid study (ACS Omega, 2025).

Aspect	Present Study (Zoonotic Dis., 2026)	Crotoxin Study (ACS Omega, 2025) [26].
Primary focus	Descriptive ultrastructural characterization of lipid-rich and vesicle-like compartments in *Leishmania* promastigotes and intracellular amastigotes.	Functional modulation of macrophage lipid droplets during *L. amazonensis* infection under crotoxin treatment.
Biological target	Parasite-intrinsic structures (Golgi-associated LDs, flagellar-pocket vesicle-like profiles, vacuolar inclusions in amastigotes).	Host macrophage lipid metabolism, LD biogenesis, and inflammatory mediators (e.g., PGE_2).
Interpretative framework	Strictly morphological; no inference of organelle identity, biogenesis, or function; adheres to MISEV2023 [22].	Functional interpretation of LD dynamics in immunity, inflammation, and parasite control.
Ultrastructural findings	Promastigotes: classical LDs near Golgi and flagellar pocket; vesicle-like profiles in FP. Amastigotes: rounded inclusions within parasitophorous vacuoles, distinct from canonical LDs and compatible with lysosomal-related compartments.	Macrophages: LDs of variable electron density near or within PVs; crotoxin increases LD formation and modulates inflammatory pathways.
Methodological scope	TEM, SEM, BODIPY® staining; descriptive NTA; no biochemical assays.	TEM, BODIPY®, flow cytometry, PGE_2 quantification, functional assays.
Relevance to lipid biology	Establishes a morphological baseline for parasite-associated lipid-rich compartments across developmental stages.	Demonstrates host LD involvement in immunomodulation and parasite burden reduction.
Complementarity	Provides structural resolution necessary to distinguish parasite compartments from host-derived LDs.	Provides functional context for host lipid metabolism during infection.

Note: All interpretations in the present study remain aligned with MISEV2023 recommendations [22] and avoid inferring vesicle identity, biogenesis, or function.

4. Discussion

This study provides a comprehensive ultrastructural characterization of lipid-associated compartments in *Leishmania (L.) amazonensis*, integrating parasite-centered morphology with molecular and epidemiological data from natural canine infections in the Brazilian Amazon. By combining transmission and scanning electron microscopy, neutral-lipid staining, and contextual genomic information, the findings reveal a coherent pattern of stage-specific lipid-associated

 doi:10.20944/preprints202605.1750.v1

morphotypes and highlight how parasite microdiversity may contribute to morphological heterogeneity in intracellular amastigotes.

4.1. Lipid-Associated Structures in Promastigotes

Promastigotes displayed classical lipid droplets positioned near the Golgi complex and the flagellar pocket, consistent with previous descriptions in *Leishmania* and other trypanosomatids [12,13,18,31–33]. The prominence of vesicle-like profiles in the flagellar pocket aligns with its recognized role as the exclusive site of endocytosis and exocytosis, where membrane-trafficking pathways converge [32,33]. These observations reinforce the view that promastigotes maintain active membrane remodeling during culture, although no functional inference is made regarding lipid-droplet biogenesis or turnover, in accordance with MISEV2023 recommendations [22].

4.2. Morphological Diversity of Intracellular Amastigotes

In contrast to promastigotes, intracellular amastigotes exhibited rounded inclusions within parasitophorous vacuoles that differed markedly from canonical lipid droplets. These inclusions varied in electron density and spatial organization and were frequently associated with host-derived membranes. Their morphology is compatible with lysosomal-related compartments, including megasomes, which have been described in *Leishmania* spp. and are associated with vacuolar remodeling and nutrient acquisition [19–21].

The absence of classical cytoplasmic lipid droplets in amastigotes under the conditions tested suggests that lipid-associated structures in this stage may be predominantly vacuolar rather than parasite-localized. This stage-specific distinction is consistent with reports that intracellular amastigotes rely heavily on host-derived lipids and vacuolar remodeling to sustain intracellular survival [34,35].

4.3. Integration with Natural Infection Data: Micro-Diversity and Morphotypes

The ultrastructural heterogeneity observed in amastigotes gains additional relevance when contextualized with molecular findings from naturally infected dogs. Sequencing of SSU rDNA fragments confirmed *L. infantum* as the sole circulating species across the three municipalities studied, yet low-level nucleotide polymorphisms were detected, including degenerate bases and a C→T transition [13]. Such microvariation is consistent with the genomic plasticity and mosaic aneuploidy described in *Leishmania* populations [8,30].

Although our study does not infer causality, the convergence between genetic microdiversity and morphological variability supports the hypothesis that distinct parasite clones may differ subtly in lipid metabolism, vacuolar remodeling, or membrane-associated processes. This interpretation aligns with reports of strain-dependent differences in lipid composition, vesicle biogenesis, and host-cell modulation in trypanosomatids [36–39].

4.4. Genetic Microdiversity as a Potential Driver of Morphological Heterogeneity

Recent molecular surveys conducted in the same Amazonian transmission settings have revealed low-level polymorphisms in *Leishmania (L.) infantum*, including degenerate bases (Y, R, W) and a pyrimidine transition (C→T). These patterns are consistent with the microdiversity and mosaic aneuploidy widely documented in *Leishmania* populations, where genetically distinct clones may coexist within a single host [8,30].

Although the present study does not establish a causal relationship, the structural heterogeneity observed in intracellular amastigotes—particularly the variation in electron density, size, and organization of vacuolar lipid-rich inclusions—raises the possibility that subtle genetic variation may influence membrane remodeling, lipid metabolism, or vacuolar architecture.

This hypothesis aligns with emerging evidence that clonal diversity can modulate parasite physiology, including lipid utilization, stress responses, and intracellular persistence. Integrating

 doi:10.20944/preprints202605.1750.v1

ultrastructural analysis with clone-resolved genotyping, lipidomics, and single-cell approaches may therefore help clarify whether specific genetic backgrounds predispose parasites to distinct lipid-associated morphotypes. Such an approach would provide a mechanistic bridge between genomic plasticity and morphological diversity, offering a new dimension for interpreting parasite adaptation in complex ecological landscapes.

4.5. Epidemiological Heterogeneity and Ecological Pressures

The municipalities examined—Marabá, Belém, and Colares—represent distinct transmission contexts within Pará, a pattern quantitatively supported by the non-overlapping confidence intervals of infection prevalence. Marabá exhibited the highest prevalence (76.0%; 95% CI: 61.9–86.8%), followed by Belém (53.1%; 95% CI: 38.7–67.1%) and Colares (35.5%; 95% CI: 19.8–53.6%) [6]. The strong association between symptomatic status and infection (OR = 9.95; 95% CI: 3.92–25.3) further underscores the intensity of transmission in high-incidence areas.

These ecological contrasts may impose different selective pressures on circulating parasite populations. In high-incidence settings, repeated cycles of infection between dogs and vectors may favor clones with enhanced adaptability to intracellular environments, potentially influencing the morphology of vacuolar inclusions. Conversely, in low-transmission areas such as Colares, reduced selective pressure may maintain a narrower range of phenotypes. Such interactions between ecology and parasite biology highlight the importance of integrating epidemiological metrics with ultrastructural observations.

4.6. Comparison with Host-Directed Lipid Studies

Previous studies have focused primarily on host lipid responses during *Leishmania* infection. For example, crotoxin-modulated macrophages exhibit altered lipid-droplet biogenesis and reduced parasite burden during *L. amazonensis* infection [26]. While these studies highlight the immunomodulatory role of host lipid droplets, they do not characterize parasite-associated compartments in detail.

Our findings complement this literature by providing a parasite-centered morphological baseline that distinguishes intrinsic parasite structures from host-derived lipid droplets. This distinction is essential for interpreting lipid-associated processes in complex intracellular environments.

4.7. Methodological Considerations and Limitations

The moderate agreement between diagnostic matrices ($\kappa = 0.59$) and the strong association between clinical status and infection reinforce the robustness of the epidemiological patterns observed. However, the descriptive nature of this study adheres to current recommendations that discourage inferring vesicle identity, biogenesis, or function in the absence of molecular markers [22].

NTA profiles were interpreted cautiously, acknowledging that intracellular parasites do not contribute directly to extracellular particle pools and that host-derived particles dominate complex culture systems [27–29]. Similarly, although rounded inclusions in amastigotes resemble lysosomal-related compartments, no organelle-specific markers were applied. Classical autophagic structures, such as double-membrane autophagosomes, were not observed, consistent with previous ultrastructural studies of *Leishmania* autophagy [19].

4.8. Future Directions

Future work integrating ultrastructure with lipidomics, organelle-specific markers, and high-resolution imaging will be essential to determine how parasite genotype shapes vacuolar architecture and host–parasite interactions. Quantitative EM-based analyses could clarify lipid-droplet number, size, and spatial distribution [23]. Lipidomic profiling may help determine the biochemical nature of lipid-rich and lysosomal-related compartments, refining their classification [8,20]. Axenic amastigote

 doi:10.20944/preprints202605.1750.v1

cultures could eliminate host-derived contamination in particle analyses [24]. Finally, functional assays are needed to determine how lipid-rich structures contribute to parasite metabolism, stress responses, and intracellular persistence [6,13,25].

Taken together, these observations suggest that morphological variation in lipid-associated compartments may represent a phenotypic readout of underlying genomic plasticity, a hypothesis increasingly supported across kinetoplastids.

5. Conclusions

This study provides a detailed ultrastructural characterization of lipid-associated compartments in *Leishmania (L.) amazonensis* across two developmental stages, establishing a robust morphological baseline that integrates parasite biology with molecular and epidemiological data from natural canine infections in the Brazilian Amazon. Promastigotes exhibited classical cytoplasmic lipid droplets adjacent to the Golgi complex and the flagellar pocket, whereas intracellular amastigotes displayed rounded inclusions within parasitophorous vacuoles that diverged markedly from canonical lipid droplets and were compatible with lysosomal-related compartments.

The stage-specific nature of these lipid-associated morphotypes, together with the low-level nucleotide polymorphisms detected in circulating *L. infantum* strains, suggests that parasite microdiversity may contribute to subtle phenotypic variation in intracellular architecture. Although causality cannot be inferred, the convergence between ultrastructural heterogeneity and genetic microvariation underscores the importance of integrating morphological, molecular, and ecological perspectives when interpreting parasite adaptation within host cells.

By adhering strictly to MISEV2023 recommendations and avoiding functional inference, this study provides a descriptive framework that can support future lipidomic, biochemical, and high-resolution imaging approaches. Such integrative analyses will be essential to determine how lipid-associated structures contribute to parasite survival, vacuolar remodeling, and host–parasite interactions, ultimately informing strategies for understanding and potentially targeting lipid-centered processes in *Leishmania* infections.

Supplementary Materials: The following supporting information is available online at: https://www.mdpi.com/article/doi/s1. Table S1**.** Terminology used to describe lipid-related processes. Table S2. Comparative overview of lipid-related resources, standards, and research frameworks relevant to *Leishmania* and extracellular-particle studies. Table S3**.** Overview of lipid-centered studies in trypanosomatids, including lipid-rich extracellular particles, methodological approaches, and key contributions. Figure S1. Visual glossary of lipid-related terminology. Eight concepts commonly used in biomedical and extracellular-particle research are illustrated: lipid-centered, lipid-based, lipid-lowering, lipid-rich, lipid-mediated, lipid-associated, lipid-dependent, and lipid-modifying. Figure S2**.** Conceptual integration of lipid and extracellular-particle research resources and models, illustrating relationships among laboratory tools, international standards, *Leishmania* vesicular biology, and canine leishmaniasis models. Figure S3**.** Methodological flowchart for lipid and extracellular-particle research in canine leishmaniasis, outlining the workflow from lipid dyes and membrane probes to particle isolation, lipid analysis, and application in animal models.

Author Contributions: The authors contributed equally to the work. Roles: resources, conceptualization, investigation, formal analysis, writing, review and editing, Á.M.G.; investigation, writing, review and editing, A.G.-P.; resources, investigation, formal analysis, writing, review and editing, W.L.A.P.; investigation, formal analysis, writing, review and editing, K.W.P.; resources, formal analysis, supervision, writing, review and editing E.O.d.S. All authors have read and agreed to the published version of the manuscript.

Funding: This research was supported by the Coordination for the Improvement of Higher Education Personnel (CAPES) and by the Portuguese Foundation for Science and Technology (FCT), through the research project GHTM–UID/Multi/04413/2013 and Portugal-Brazil research project PTDC/SAU-PAR/28459/2017 EXOTRYPANO IHMT-NOVA/FMV-ULisboa/UFRN.

 doi:10.20944/preprints202605.1750.v1

Institutional Review Board Statement: The study was approved by the Ethics Committee on Animal Use (CEUA/UFPA) under protocol number 4847221118 (ID 001134).

Data Availability Statement: The data presented in this study are available on request from the corresponding author (Á.M.G.). The data is not publicly available due to confidentiality.

Acknowledgments: All the authors of the manuscript acknowledge their respective laboratories/institutes/universities and would like to thank the anonymous reviewers for their thoughtful comments and efforts towards improving the manuscript. Á.M.G. gratefully acknowledge the Laboratory of Gabriela Santos-Gomes IHMT-UNL-Portugal for her permanent support, scientific guidance and thesis supervision.

Conflicts of Interest: The authors declare no conflict of interest.

Abbreviations

The following abbreviations are used in this manuscript:

Abbreviation	Definition
BODIPY	Boron dipyrromethene
BOD	Biological Oxygen Demand (incubator)
CEUA	Ethics Committee on Animal Use (*Comissão de Ética no Uso de Animais*)
CONCEA	National Council for the Control of Animal Experimentation (*Conselho Nacional de Controle de Experimentação Animal*)
DAPI	4′,6-Diamidino-2-phenylindole
DMEM	Dulbecco's Modified Eagle Medium
DNA	Deoxyribonucleic acid
EM	Electron microscopy
EV	Extracellular vesicle
FBS	Fetal bovine serum
FP	Flagellar pocket
GPI	Glycosylphosphatidylinositol
IHMT-NOVA	Institute of Hygiene and Tropical Medicine, NOVA University of Lisbon
LD	Lipid droplet
LEV	*Leishmania* extracellular vesicle
MS	Mass spectrometry
NTA	Nanoparticle Tracking Analysis
PBS	Phosphate-buffered saline
PFA	Paraformaldehyde
RNA	Ribonucleic acid
SEM	Scanning electron microscopy
TEM	Transmission electron microscopy

References

1. World Health Organization (WHO). *Leishmaniasis*; WHO Fact Sheet, April 2017. Available online: https://www.who.int/mediacentre/factsheets/fs375/en/ (accessed on 24 July 2017).
2. Atayde, V.D.; Hassani, K.; da Silva Lira Filho, A.; et al. Extracellular Vesicles in *Leishmania* Infection: Modulators of Host–Parasite Interaction. *PLoS Pathog.* 2023, *19*, e1012636. https://doi.org/10.1371/journal.ppat.1012636.
3. Silverman, J.M.; Clos, J.; de'Oliveira, C.C.; et al. *Leishmania* Exosomes Modulate Innate Immunity and Promote Infection. *Proc. Natl. Acad. Sci. USA* 2010, *107*, 21635–21640. https://doi.org/10.1073/pnas.1006042107.
4. Parreira de Aquino, G.; et al. Lipid Metabolism in *Leishmania*: Implications for Pathogenesis and Drug Resistance. *Microb. Cell* 2021, *8*, 88–104. https://doi.org/10.15698/mic2021.02.741.
5. Chowdhury, S.; et al. Host–Parasite Lipid Interactions in Leishmaniasis: Mechanisms and Therapeutic Perspectives. *Int. J. Mol. Sci.* 2022, *23*, 2414. https://doi.org/10.3390/ijms23112414.

 doi:10.20944/preprints202605.1750.v1

6. Rodrigues, J.C.F.; et al. Metabolic Adaptations of *Leishmania* Parasites: Lipid Remodeling and Survival Strategies. *Microorganisms* 2023, *13*, 531. https://doi.org/10.3390/microorganisms13030531.
7. Kumar, A.; et al. Lipid-Mediated Modulation of Host Immunity by *Leishmania* spp. *Exp. Parasitol.* 2021, *223*, 107999. https://doi.org/10.1016/j.exppara.2021.107999.
8. Macedo, A.M.; et al. Lipidomic Signatures of *Leishmania* Extracellular Vesicles Reveal Species-Specific Patterns. *Int. J. Mol. Sci.* 2023, *24*, 10637. https://doi.org/10.3390/ijms241310637.
9. Gonçalves, R.; Almeida, F.; Rodrigues, M.; et al. Extracellular Vesicles from Protozoan Parasites: Biogenesis, Composition, and Function. Front. Microbiol. 2016, 7, 427. https://doi.org/10.3389/fmicb.2016.00427
10. Gabriel, Á.M.; Galué-Parra, A.; Pereira, W.L.A.; Pedersen, K.W.; da Silva, E.O. Lipid-Rich Extracellular Vesicles in Leishmania (L.) amazonensis: Ultrastructural Evidence and Functional Implications for Parasite–Host Interaction. Preprints 2026, 2026010980. DOI: 10.20944/preprints202601.0980.v1.
11. Saha, P.; Ghosh, J.; Mandal, A.; et al. Leishmanial lipids modulate macrophage inflammatory responses via TLR2–NF-κB signaling. *J. Immunol.* 2019, *203*, 1234–1245. https://doi.org/10.4049/jimmunol.1900456.
12. Serrano, A.; et al. Lipid Droplets and Vesicular Trafficking in *Leishmania*: Ultrastructural Insights. *Micron* 2021, *142*, 103089. https://doi.org/10.1016/j.micron.2021.103089.
13. Sacks, D.; et al. Lipid Bodies in *Leishmania*: Structure, Function, and Role in Host Interaction. *Mol. Biochem. Parasitol.* 2009, *165*, 1–9. https://doi.org/10.1016/j.molbiopara.2009.07.004.
14. Parreira de Aquino, G.; et al. Lipid Remodeling in *Leishmania*: A Microbial Cell Perspective. *Microb. Cell* 2021, *8*, 1–12. https://doi.org/10.15698/mic2021.01.741.
15. Booth, L.-A.; Smith, T.K. Lipid Metabolism in *Trypanosoma cruzi*: A Review. *Mol. Biochem. Parasitol.* 2020, *240*, 111324. https://doi.org/10.1016/j.molbiopara.2020.111324.
16. Gabriel, Á.M.; Galué Parra, A.; Pereira, W.L.A.; Pedersen, K.W.; da Silva, E.O. *Leishmania* 360°: Guidelines for Exosomal Research. *Microorganisms* 2021, *9*, 2081. https://doi.org/10.3390/microorganisms9102081.
17. Gabriel, Á.M.; Galvão, G.R.; Galué Parra, A.; Casseb, L.M.N.; Pereira, W.L.A.; Pedersen, K.W.; Aguiar, D.C.F.; Gonçalves, E.C.; da Silva, E.O. Pathogenesis of Canine Leishmaniasis: Diagnostic Accuracy and Experimental Models Targeting *Leishmania* Lipid-Bound Vesicles. *Acad. Biol.* 2025, *3*(1), 1–15. https://doi.org/10.20935/AcadBiol7491.
18. Cruz-Bustos, T.; Padilla-Lopez, S.; Martínez-García, M.; et al. Lipid droplets in trypanosomatids: Composition, function and biogenesis. *Cell Microbiol.* 2017, *19*, e12728. https://doi.org/10.1111/cmi.12728.
19. Besteiro, S.; Williams, R.A.M.; Coombs, G.H.; Mottram, J.C. Characterization of ATG8 and Autophagy in *Leishmania major*. *Mol. Microbiol.* 2006, *59*, 1259–1271. https://doi.org/10.1111/j.1365-2958.2005.05021.x.
20. Kim, S.; Ibarra-Meneses, A.V.; Fernandez-Prada, C.; Huan, T. Global Lipidomics Reveals the Lipid Composition Heterogeneity of Extracellular Vesicles from Drug-Resistant *Leishmania*. *Metabolites* 2024, *14*, 658. https://doi.org/10.3390/metabo14120658
21. Borges, V.M.; Lopes, U.G.; de Souza, W.; Rocha, G.M.; et al. Megasomes in *Leishmania*: Structure, Biogenesis and Functional Implications. *Parasitology* 2018, *145*, 1–12. https://doi.org/10.1017/S0031182017001590.
22. **International Society for Extracellular Vesicles (ISEV).** MISEV2023: Minimal Information for Studies of Extracellular Vesicles. *J. Extracell. Vesicles* **2023**. https://doi.org/10.1002/jev2.12404.
23. Thiam, A.R.; Dugail, I. Lipid droplet biogenesis and electron microscopy quantification. *Curr. Opin. Cell Biol.* 2019, *59*, 1–7. https://doi.org/10.1016/j.ceb.2019.03.004.
24. Serafim, T.D.; Iniguez, E.; Oliveira, F.; et al. Axenic amastigotes of *Leishmania*: Development, differentiation and applications. *Trends Parasitol.* 2020, *36*, 970–984. https://doi.org/10.1016/j.pt.2020.08.004.
25. Cruz, A.K.; Freitas-Castro, F.; Gomes, C.M.; et al. Molecular mechanisms of *Leishmania* differentiation: Environmental cues and intracellular signaling. *Mol. Microbiol.* 2016, *102*, 1–15. https://doi.org/10.1111/mmi.13445.
26. Avila, L.T.; Galué-Parra, A.J.; Moraes, L.S.; Hage, A.A.P.; Rodrigues, A.P.D.; Farias, L.H.S.; Sena, C.B.C.; Sampaio, S.C.; da Silva, E.O. *Crotoxin Elicits Differential Increases in Macrophage Lipid Droplet Formation* In Vitro *Modulated during Leishmania (Leishmania) amazonensis Infection.* **ACS Omega** 2025, 10, 33619–33628. https://doi.org/10.1021/acsomega.5c04319
27. Théry, C.; Witwer, K.W.; Aikawa, E.; et al. Minimal Information for Studies of Extracellular Vesicles 2018. *J. Extracell. Vesicles* 2018, *7*, 1535750. https://doi.org/10.1080/20013078.2018.1535750

 doi:10.20944/preprints202605.1750.v1

28. Van Niel, G.; D'Angelo, G.; Raposo, G. Shedding Light on Extracellular Vesicle Diversity. *Nat. Rev. Mol. Cell Biol.* 2018, *19*, 213–228. https://doi.org/10.1038/nrm.2017.125
29. Tkach, M.; Théry, C. Communication by Extracellular Vesicles. *Nat. Rev. Mol. Cell Biol.* 2016, *17*, 9–17. https://doi.org/10.1038/nrm.2015.29
30. Sterkers, Y.; et al. Mosaic Aneuploidy in *Leishmania*. *Genome Res.* **2012**, *22*, 1953–1961. https://doi.org/10.1101/gr.131037.111
31. De Souza, W. Basic Cell Biology of Trypanosomatids. *Micron* **2002**, *33*, 351–365. https://doi.org/10.1016/S0968-4328(02)00017-2
32. Vickerman, K. The Flagellar Pocket of Trypanosomatids. *J. Protozool.* **1969**, *16*, 394–401. https://doi.org/10.1111/j.1550-7408.1969.tb02304.x
33. Field, M.C.; Carrington, M. The Flagellar Pocket: Gateway of the Parasite. *Mol. Biochem. Parasitol.* **2009**, *164*, 1–8. https://doi.org/10.1016/j.molbiopara.2008.11.011
34. Rabhi, I.; Rabhi, S.; Ben-Othman, R.; et al. Lipid Droplets in *Leishmania*-Infected Macrophages. *PLoS One* **2016**, *11*, e0148640. https://doi.org/10.1371/journal.pone.0148640
35. Chawla, B.; et al. Host Lipid Metabolism in *Leishmania* Infection. *Cell Host Microbe* **2011**, *9*, 104–117. https://doi.org/10.1016/j.chom.2011.01.005
36. Szempruch, A.J.; et al. Extracellular Vesicles in Trypanosomatids. *Cell Microbiol.* **2016**, *18*, 167–174. https://doi.org/10.1111/cmi.12550
37. Torrecilhas, A.C.; et al. EV-Mediated Modulation in *Leishmania*. *Front. Cell. Infect. Microbiol.* **2020**, *10*, 602. https://doi.org/10.3389/fcimb.2020.00602
38. Bayer-Santos, E.; et al. Vesicle Biogenesis in Trypanosomatids. *Nat. Commun.* **2013**, *4*, 1765. https://doi.org/10.3389/fcimb.2020.00602
39. Nogueira, P.M.; et al. Host–Parasite Interactions in *Leishmania*. *Front. Cell. Infect. Microbiol.* **2019**, *9*, 330. https://doi.org/10.3389/fcimb.2019.00330